

Tamás Soháda<sup>1</sup>  
Wen Hui Hu<sup>2</sup>  
Li Li Zeng<sup>2</sup>  
Hong Li<sup>2</sup>  
Lajos Szente<sup>3</sup>  
Béla Noszál<sup>1</sup>  
Szabolcs Béni<sup>1</sup>

<sup>1</sup>Semmelweis University,  
Department of Pharmaceutical  
Chemistry, Budapest, Hungary  
<sup>2</sup>Guangzhou Institutes of  
Biomedicine and Health,  
Chinese Academy of Sciences,  
Guangzhou, P. R. China  
<sup>3</sup>Cyclolab Ltd., Budapest,  
Hungary

Received December 1, 2010  
Revised February 17, 2011  
Accepted February 24, 2011

## Research Article

# Evaluation of the interaction between sitagliptin and cyclodextrin derivatives by capillary electrophoresis and nuclear magnetic resonance spectroscopy

An aqueous capillary electrophoretic method was developed for chiral analysis of the novel anti-diabetic drug, sitagliptin. The acid–base profiling of the analyte was carried out using both capillary electrophoresis and nuclear magnetic resonance pH titrations. The apparent complex stability and chiral separation properties were investigated with 30 different cyclodextrins under acidic conditions. The effect of concentration and pH of the BGE, temperature of the capillary, and the type and concentration of the chiral selector on the enantiomer resolution were thoroughly investigated. The effects of dual cyclodextrin systems on separation were also extensively studied. Complete separation of racemic sitagliptin with good resolution ( $R_S = 2.24$ ) was achieved within a short time (15 min) with optimized parameters (10°C, pH = 4.4, 40 mM phosphate buffer) of a sulfobutylether- $\beta$ -cyclodextrin (averaged degree of substitution  $\sim 4$ ) and native  $\beta$ -cyclodextrin dual system. The averaged stoichiometry of the inclusion complex was determined using the Job plot method with both  $^1\text{H}$  and  $^{19}\text{F}$  NMR experiments and resulted in a 1:1 complex. The structure of the inclusion complex was elucidated using 2-D ROESY NMR experiments.

### Keywords:

$^{19}\text{F}$  NMR / Dual cyclodextrin / Enantioseparation / Januvia / Sitagliptin synthesis  
DOI 10.1002/elps.201000639

## 1 Introduction

Sitagliptin (Sgli) (Fig. 1), (*R*)-4-oxo-4-[3-(trifluoromethyl)-5,6-dihydro[1,2,4]triazolo[4,3-*a*]pyrazin-7(8H)-yl]-1-(2,4,5-trifluorophenyl)butan-2-amine (formerly MK-0431, Javunia<sup>®</sup>, Merck), an orally active, potent, and highly selective inhibitor of dipeptidyl peptidase-4, has recently been approved in the United States for the treatment of type 2 diabetes [1]. Sgli increases glucose-dependent insulin secretion, decreases abnormal glucagon secretion, decelerates stomach motion, increases  $\beta$ -cell number, and reduces appetite [2–5].

**Correspondence:** Dr. Szabolcs Béni, Department of Pharmaceutical Chemistry, Semmelweis University, Hőgyes Endre u. 9., H-1092 Budapest, Hungary  
**E-mail:** beniszabi@gytk.sote.hu  
**Fax:** +36-1-217-0891

**Abbreviations:** **CE- $\beta$ -CD**, carboxyethylated- $\beta$ -CD sodium salt; **DS**, degree of substitution (number of substituted hydroxyl groups per CD); **HP- $\beta$ -CD**, (2-hydroxy)propyl- $\beta$ -CD; **ROESY**, rotating frame nuclear Overhauser effect spectroscopy; **SB- $\alpha$ -CD**, sulfobutyl-ether- $\alpha$ -CD sodium salt; **SB- $\beta$ -CD**, sulfobutyl-ether- $\beta$ -CD sodium salt; **Sgli**, sitagliptin; **SP- $\alpha$ -CD**, sulfopropylated- $\alpha$ -CD sodium salt

Sgli was quantified in human plasma using protein precipitation and tandem mass spectrometry (LC-MS/MS) by Zeng et al. [6] and using liquid–liquid extraction and MS/MS (LC-MS/MS) by Nirogi et al. [7].

A wide range of synthetic procedures were developed to synthesize Sgli and its precursors [1, 8–12]. Some of these methods carry the possibility of enantiomeric contamination with the undesired (*S*)-enantiomer of enantiopure Sgli, and therefore enantioselective analytical methods are necessary to control the enantiomeric purity of pharmaceutical Sgli preparations.

CE is a frequently used technique for enantioseparation of chiral compounds. CE has gained a significant degree of acceptance in the analytical laboratories owing to its many advantages such as high efficiency, high resolution, rapid analysis, and low consumption of samples and reagents. Among the chiral selectors, CDs represent an eminent class to achieve and optimize the separation of enantiomers via complexation [13, 14]. Chiral recognition using CDs is based on the different interaction affinities between the chiral selector and the analyte enantiomers. Charged CDs and particularly sulfated CDs (with or without an alkyl spacer) are widely used for the enantioseparation of either neutral or cationic analytes [15]. In this last case, CDs provide additional electrostatic interactions and higher enantioresolutions which are mainly due to the enhanced mobility

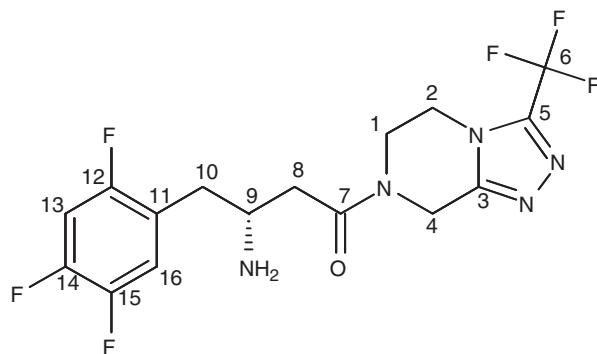


**Figure 1.** The chemical structure and numbering of (*R*)-Sgli.

difference between the free and the complexed analyte [16, 17]. Several articles have been recently published on the improvement of enantioseparations using sulfated CDs in dual systems (combination of neutral and ionized CDs) [18, 19]. A large number of experimental parameters influence the unpredictable enantioselectivity and the performance of a CD-based CE method. The classical optimization parameters are the nature and concentration of the CD, the composition of the BGE (pH, concentration of the buffer, addition of organic modifier), the separation voltage, and the capillary temperature.

Concerning the various methods to study inclusion complexation, NMR spectroscopy is certainly a powerful one. It allows the quantitation of the host–guest equilibria [20] in terms of stability constant with a dynamic range from  $10$  to  $10^4$  [21, 22]. The simultaneous incorporation of data-sets of several nuclei into the set of equations results in robust estimates of apparent averaged stability constants. It is also a reliable tool to determine complex stoichiometry [22–24] and reveal the geometry of the diastereomeric complex [20, 22, 25, 26].

To the best of our knowledge, no chiral separation method of Sgli has been reported despite the numerous articles discussing the structure–activity relationships of this molecule. Here, we report a CD-based, fast, and reliable CE method for the separation of Sgli enantiomers and a thorough investigation of the complexation behavior.

## 2 Materials and methods

### 2.1 Chemicals

(*R*)- and (*S*)-4-oxo-4-[3-(trifluoromethyl)-5,6-dihydro[1,2,4]-triazolo[4,3-*a*]pyrazin-7(8H)-yl]-1-(2,4,5-trifluorophenyl)butan-2-amine were synthesized as published earlier [11]. The full  $^1\text{H}$  and  $^{13}\text{C}$  NMR assignment is included in Table 1. Both analytes were dissolved in MeOH and kept at  $-20^\circ\text{C}$ . All native CDs and their derivatives were the products of Cyclolab (Budapest, Hungary). During CE experiments, all native ( $\alpha$ ,  $\beta$ ,  $\gamma$ ) CDs, their trimethylated, 2-hydroxypropylated, sulfopropylated, and sulfobutylated derivatives, randomly and dimethylated-, acetylated-, 6-monoamino-

**Table 1.**  $^1\text{H}$  and  $^{13}\text{C}$  NMR assignment of Sgli in  $\text{CD}_3\text{OD}$  (TMS as reference  $\delta = 0.000$  ppm)

No.	$^{13}\text{C}$	$^1\text{H}$	m, J (Hz), int.
1	41.1	4.17–4.23 3.95–4.04	m, 1H m, 1H
2	43.6	4.28	m, 1H m, 1H
3	151.3		
4	38.3	4.91 5.03	d, 17.7, 1H d, 17.7, 1H
5	155.6–157.2		
6	42.1		
7	171.2		
8	38.7	2.50–2.65	m, 2H
9	48.4	3.45–3.53	m, 1H
10	35.1	2.73–2.83	m, 2H
11	130.9		
12	121.2–123.3		
13	105.2	7.08–7.15	m, 1H
14	147.4–149.6		
15	145.7–148.0		
16	119.2	7.24–7.29	m, 1H

6-monodeoxy-, succinylated-, carboxymethylated-, carboxymethylated-, phosphated- and sulfo(2-hydroxy)-propylated- $\beta$ -CDs and carboxymethylated- and sulfo(2-hydroxy)-propylated- $\gamma$ -CDs were used.  $\text{H}_3\text{PO}_4$ ,  $\text{NaH}_2\text{PO}_4 \cdot \text{H}_2\text{O}$ ,  $\text{Na}_2\text{HPO}_4 \cdot 2\text{H}_2\text{O}$ , NaOH, and HCl used for the preparation of BGE of analytical grade were purchased from commercial suppliers. The NMR solvents  $\text{D}_2\text{O}$  (>99.8 atom % D) and  $\text{CD}_3\text{OD}$  were obtained from Sigma. As EOF marker in CE experiments DMSO from Reanal (Budapest, Hungary) was used. All reagents were used without further purification. Bidistilled Millipore water was used throughout this study. NMR spectra were processed with MestreNova 5.3.1-4825 software.  $\text{pK}_a$  values were determined with OPIUM computer program (1995).

### 2.2 CE

All CE experiments were performed on a  $^3\text{D}$ CE instrument (Agilent Technologies, Waldbronn, Germany), equipped with a photodiode array detector. Instrument control, data acquisition, and data analysis were performed by the HP $^3\text{D}$  CE ChemStation software. An untreated fused silica capillary (50  $\mu\text{m}$  id, 64.5 cm total, 56 cm effective length) was purchased from Agilent. Conditioning of new capillaries was conducted by flushing with 1 M NaOH for 30 min followed by 0.1 M NaOH and buffer for 60 min each. During measurements, +30 kV voltage was applied and the capillary was thermostated at 298 K, unless stated otherwise. UV detection was performed at 200, 215, 220, 225, and 230 nm and samples were run in triplicate. Along with the UV traces, the current and the voltage were monitored. Prior to all runs, the capillary was preconditioned by rinsing with

water (2 min), 0.1 M NaOH (1 min), water (1 min), and BGE (2 min). The samples were injected hydrodynamically (200 mbar\*s). During the preliminary experiments, the pH of a 30 mM phosphate buffer was set to 6.0 with NaOH. The stock solution of Sgli (containing 0.1 mM of each enantiomer) contained 1% v/v MeOH and 0.1% v/v DMSO, the latter served as EOF marker.

As primary response functions  $t_{\text{EOF}}$ ,  $t_1$ , and  $t_2$  migration times were recorded. Effective mobility values were calculated as follows:

$$\mu_{\text{eff}} = \frac{l_c l_d}{U} \cdot \left( \frac{1}{t} - \frac{1}{t_0} \right) \quad (1)$$

where  $l_c$  is the total length of the capillary,  $l_d$  is the length of the capillary to the detector,  $U$  is the applied voltage, and  $t$  and  $t_0$  are the peak appearance times of the analyte and the EOF, respectively [27]. Apparent averaged complex stability constants were determined according to the  $x$ -reciprocal method by plotting the data in the form  $(\mu_{\text{eff}} - \mu_{\text{free}})/[\text{CD}]$  versus  $(\mu_{\text{eff}} - \mu_{\text{free}})$ , yielding  $-K$  as the slope [28]. The concentration of the CDs varied from 1 to 50 mM during preliminary experiments. The resolution ( $R_s$ ) was calculated as the secondary response function when evaluating the performance of the separation system.

### 2.3 NMR spectroscopy

$^1\text{H}$  and  $^{13}\text{C}$  NMR experiments were carried out on a Varian VNMRs (600 MHz for  $^1\text{H}$ ) spectrometer equipped with a dual 5-mm inverse-detection gradient (IDPF) probehead, whereas  $^{19}\text{F}$  NMR data were recorded on a Varian Mercury Plus spectrometer (400 MHz for  $^1\text{H}$ ). In case of structure identifications, standard pulse sequences and processing routines available in Vnmrj 2.2C/Chempack 4.0 were used.  $^1\text{H}$  and  $^{13}\text{C}$  chemical shifts in  $\text{CD}_3\text{OD}$  were referenced to internal TMS ( $\delta = 0.000$  ppm). In total, 700  $\mu\text{L}$  of solutions were introduced into standard 5 mm NMR tubes and the spectra were performed at 298 K. The  $^1\text{H}$  NMR-pH titration was carried out in a 0.1 M NaCl, 30 mM phosphate solution (ionic strength kept constant) at pH ranging from 6.23 to 10.15 in  $\text{H}_2\text{O}/\text{D}_2\text{O}$  9/1. As reference DSS ( $\delta = 0.000$  ppm) was used. The titrants (0.1 M HCl or 0.1 M NaOH) were added in small portions (5–20  $\mu\text{L}$ ) from a Hamilton syringe and the samples were homogenized afterward. To confirm the averaged stoichiometry of the inclusion complex between Sgli and  $\beta$ -CD (MW = 1135), sulfobutyl-ether- $\beta$ -CD sodium salt (SB- $\beta$ -CD) (DS~4, MW = 1767.7) (DS, degree of substitution [number of substituted hydroxyl groups per CD]) and  $\beta$ -CD/SB- $\beta$ -CD (1/1) dual CD system, the method of continuous variation (Job plot analysis) [23] was used. The total concentration of the interacting species ((*R*)-Sgli and  $\beta$ -CD/SB- $\beta$ -CD) was kept constant at 4 mM in 30 mM phosphate buffer (in  $\text{H}_2\text{O}/\text{D}_2\text{O}$  9/1). For molarity calculations, water content of  $\beta$ -CD (13.4%) and SB- $\beta$ -CD (4.3%) were taken into consideration.  $^1\text{H}$  NMR spectra were referenced to the residual methanol signal (3.300 ppm), with

the advantage of a reference without any significant interaction with CDs in minute concentrations. The molar fraction  $x$  ( $x = [\text{analyte}]/([\text{analyte}] + [\text{CD}]$  or  $x = [\text{CD}]/([\text{analyte}] + [\text{CD}])$ ) varied in the range of 0–1 by 0.1 steps. During  $^1\text{H}$  NMR experiments, 32–256 scans (depending on the experiment) with a spectral window of 5400 Hz were collected into 64 000 data points, giving a digital resolution of 0.08 Hz/point. For solvent signal suppression, the dpfsg\_water pulse sequence was used. In case of  $^{19}\text{F}$  NMR for Job plot experiments NaF ( $\delta = -122.000$  ppm) was used as internal reference. The average extent of penetration and the direction of inclusion were investigated by 2-D phase sensitive rotating frame nuclear Overhauser effect spectroscopy (ROESY). In the case of inclusion complex formation, the guest penetrates the cavity of the CD derivative where spatial proximities can be detected between the inner cavity CD protons (H-3 and H-5) and the appropriate protons of the guest using NMR. Stock solution for ROESY experiments contained 5 mM (*R*)-Sgli and 30 mM  $\text{NaH}_2\text{PO}_4$  in  $\text{D}_2\text{O}$ . Three samples were then prepared by adding either 3 mM  $\beta$ -CD or 3 mM SB- $\beta$ -CD or 2.2 mM  $\beta$ - and SB- $\beta$ -CD to the stock solution. The spectra were recorded applying various mixing times of 200, 300, and 500 ms on all three samples. A total of 512 increments were collected with 24 repetitions and the measured data matrix was processed as a matrix of 4K (F2) by 1K (F1) data points. Intermolecular NOEs between Sgli and CD protons directly involved in the host-guest interaction were detected as cross-peaks.

## 3 Results and discussion

### 3.1 Acid–base profiling

#### 3.1.1 CE–pH titration

The electrophoretic study of Sgli–CD complexation requires the acid–base profiling of the molecule. To determine the binding constants and study the enantioseparation properties of neutral CDs, the analyte must be in protonated form, as a positive ion. The titration was carried out in the pH range of 2.01–10.56, applying the parameters mentioned in Section 2.2. The effective mobility values were calculated and plotted as a function of pH. The observed electrophoretic mobility at a particular pH is a weighted sum of individual mobilities of the unprotonated ( $\mu_{\text{Sgli}}$ ) and protonated ( $\mu_{\text{HSgli}^+}$ ) form of the molecule, which can be rearranged to the master equation of  $\text{p}K_a$  determination by CE. A curve was fitted on the observed data points using the following equation [29]:

$$\mu_{\text{eff}} = \frac{\mu_{\text{Sgli}} + \mu_{\text{HSgli}^+} \cdot 10^{\text{p}K_a - \text{pH}}}{1 + 10^{\text{p}K_a - \text{pH}}} \quad (2)$$

For the amino group of Sgli,  $\text{p}K_a = 7.61 \pm 0.07$  was determined. This constant is lower than the expected one of a primary amino function. The weaker basicity of the group can be explained by the vicinity of the electron-withdrawing

trifluor-aromatic ring and the possibility of hydrogen bonding between the amino- and the carbonyl groups. The pH values applied in subsequent experiments were set upon this constant, considering that at  $\text{pH} \leq (\text{p}K_a - 1)$  value the analyte is predominantly in its protonated form.

### 3.1.2 NMR–pH titration

Besides CE–pH titration, NMR–pH titration is also an effective tool for the determination of dissociation constants. Since protonation processes are rapid on the NMR time-scale, the observed chemical shifts ( $\delta^{\text{obs}}$ ) are weighted averages of the chemical shifts of the distinct protonation forms ( $\delta_{\text{SgIi}}$ ,  $\delta_{\text{HSgIi}^+}$ ):

$$\delta^{\text{obs}} = \delta_{\text{SgIi}} \alpha_{\text{SgIi}} + \delta_{\text{HSgIi}^+} \alpha_{\text{HSgIi}^+} = \frac{\delta_{\text{SgIi}} + \delta_{\text{HSgIi}^+} K_a [\text{H}^+]}{1 + K_a [\text{H}^+]} \quad (3)$$

Expressing the  $\alpha$  mole fractions in terms of pH and  $\text{p}K_a$  dissociation constant, the master equation to fit the NMR–pH titration curves is obtained [29, 30]:

$$\delta^{\text{obs}} = \frac{\delta_{\text{SgIi}} + \delta_{\text{HSgIi}^+} (10^{\text{p}K_a - \text{pH}})}{1 + 10^{\text{p}K_a - \text{pH}}} \quad (4)$$

The individual chemical shifts ( $\delta_{\text{SgIi}}$ ,  $\delta_{\text{HSgIi}^+}$ ) and the  $\text{p}K_a$  value were calculated from the  $\delta^{\text{obs}}$ –pH data sets.

The dissociation constant of SgIi was determined to be  $\text{p}K_a = 8.03 \pm 0.05$ , which is in good correlation with CE–pH results, considering the differences in experimental conditions such as composition of solvent, ionic strength, and accuracy of the method.

### 3.2 Chiral separation method development and optimization: Determination of binding constants and enantioseparation

The binding constants between the analyte and the chiral selector are of fundamental interest to understand the inclusion behavior (information on the analyte–ligand affinity and understanding the molecular interactions) [31, 32]. Several requirements must be met in order to estimate the binding constants by CE. First, the solute must experience a change in electrophoretic mobility upon interaction with the CD molecule (either inclusion complexation or interaction with the outer surface or the side chain of the CD). To fulfill this criterion, either the analyte or the selector has to exist in a charged form during the electrophoretic run. Second, the equilibrium time scale must be faster than the CE separation time scale. The last requirement means that sufficient concentrations of both free ligand and ligand–analyte complex should be present [27]. Based on the  $\text{p}K_a$  values determined by CE–pH and NMR–pH titrations, the pH of the preliminary CE experiments was set to pH 6.0. Due to Wren's theory, the optimal CD concentration for the enantioseparation can be calculated as:

$$[\text{CD}]_{\Delta\mu}^{\text{opt}} = \frac{1}{\sqrt{K_R K_S}} \quad (5)$$

where  $K_R$  and  $K_S$  are the stability constants of the inclusion complexes of the *R* and *S* enantiomer, respectively [33]. For the determination of the binding constants, various concentrations of CDs (ranging from 5 to 50 mM) were added to the BGE. The determined binding constants and enantioresolution values (calculated at the optimal concentrations according to Wren's) of the single CD systems causing enantioseparation are listed in Table 2.

It is obvious that the affinity of SgIi to most of the CDs is poor. Most of the complexes possess weak stability ( $K < 100$ ) and none of the neutral and positive CDs resulted in enantioseparation. Partial separation was achieved with six negative CDs: carboxymethylated- $\gamma$ -CD sodium salt DS~3, carboxyethylated- $\beta$ -CD sodium salt (CE- $\beta$ -CD) DS~3, sulfo-propylated- $\alpha$ -CD sodium salt (SP- $\alpha$ -CD) DS~4, sulfo(2-hydroxy)-propylated- $\beta$ -CD sodium salt DS~2.5, sulfobutyl-ether- $\alpha$ -CD sodium salt (SB- $\alpha$ -CD) DS~4, and SB- $\beta$ -CD DS~4. The best resolution ( $R_S = 1.02$ ) was reached adding 5 mM SB- $\beta$ -CD to the BGE. Representative electropherograms using optimal concentration of CE- $\beta$ -CD and SB- $\beta$ -CD are shown in Fig. 2A and B. Identification of the enantiomers was carried out by spiking the analyte with the single (*S*)-isomer. The migration order of the enantiomers (considering the charges of guest and host molecules and parameters of the run) highlights that the (*R*)-SgIi has higher affinity toward all the enantioseparating CDs than the (*S*)-enantiomer. Single CDs employed in these systems failed to provide baseline separation of racemic SgIi, and thus dual CD systems were used for further optimization.

In these systems, an ionized and a neutral CD were mixed at different concentrations. In general, with different selectivities and mobility affecting properties of the two CDs, better separation could be achieved than with the single components. Improvement of resolution was unambiguously observed in most of the applied dual CD systems, nevertheless, a real breakthrough in resolution enhancement was not observed. Twelve pairs of CDs were selected in accordance with our preliminary results. Concerning the neutral CDs, our choice was focused on the  $\beta$ -CD,

**Table 2.** Apparent binding constants ( $K$ ) and enantioseparation data ( $R_S$ )<sup>a)</sup> of SgIi–CD systems (only CDs resulting enantioseparation)

CD	Stability ( $K$ )	$R_S$
CM- $\gamma$ -CD DS~3	<i>S</i> : 120 (3) <sup>b)</sup> , <i>R</i> : 125 (4)	0.50
CE- $\beta$ -CD DS~3	<i>S</i> : 119 (4), <i>R</i> : 124 (8)	0.74
SP- $\alpha$ -CD DS~2	<i>S</i> : 48 (2), <i>R</i> : 50 (1)	0.81
SHP- $\beta$ -CD <sup>c)</sup> DS~3	<i>S</i> : 49 (2), <i>R</i> : 52 (3)	0.42
SB- $\alpha$ -CD DS~4	<i>S</i> : 312 (4), <i>R</i> : 320 (8)	0.77
SB- $\beta$ -CD DS~4	<i>S</i> : 100 (10), <i>R</i> : 115 (8)	1.02

a) The resolution stands for the resolution at optimal selector concentration according to Wren's formula.

b) Uncertainties in parentheses are estimated standard deviations of the last significant digit.

c) SHP- $\beta$ -CD, sulfo(2-hydroxy)-propylated- $\beta$ -CD sodium salt.

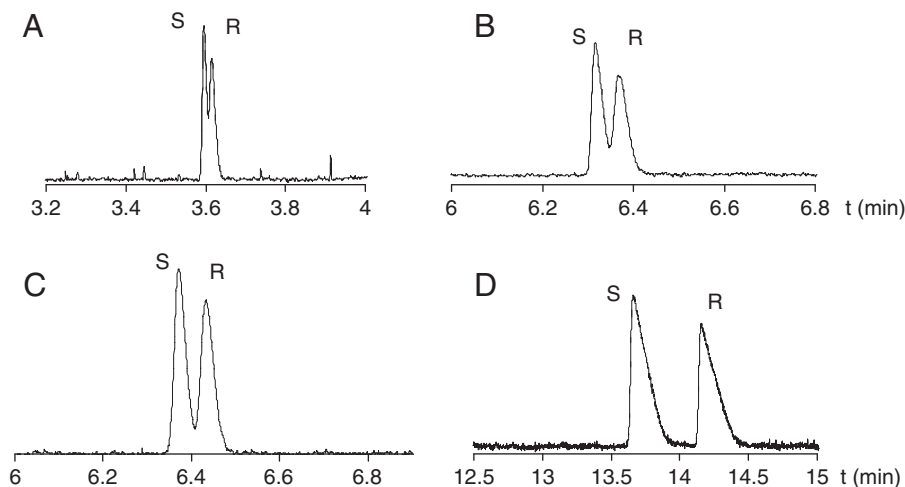


**Figure 2.** Enantioseparation of racemic Sgli with 30 mM CE- $\beta$ -CD (A), 5 mM SB- $\beta$ -CD DS~4 (B), the dual CD system of 5 mM SB- $\beta$ -CD, 15 mM HP- $\beta$ -CD (C), and the optimized separation of the enantiomers with 5 mM SB- $\beta$ -CD, 5 mM  $\beta$ -CD dual system (D). For further details, see Section 3.2.1.

(2-hydroxy)propyl- $\beta$ -CD (HP- $\beta$ -CD) (DS~6.3) and heptakis(2,6-di-*O*-methyl)- $\beta$ -CD, which allowed sufficiently strong analyte-CD complexations (compared with other neutral CDs). Concerning the anionic CDs, the four most promising, CE- $\beta$ -CD, SP- $\alpha$ -CD, SB- $\alpha$ -CD, and SB- $\beta$ -CD (DS~4) were selected. Electropherogram of 5 mM SB- $\beta$ -CD, 15 mM HP- $\beta$ -CD dual CD system is shown in Fig. 2C.

The best result was achieved with the 5 mM SB- $\beta$ -CD, 5 mM native  $\beta$ -CD system resulting in baseline separation ( $R_s = 1.51$ ) without further optimization. For an even better separation, three basic parameters such as pH, buffer concentration, and temperature were optimized for the dual CD system. During the optimization, single variation method was used, and thus the effect of one parameter only was observed at a time. The effect of pH was monitored in the range of 3.90–6.17 by approx. 0.25 pH steps, and the concentration of phosphate buffer was investigated in the range of 10–50 mM by 10 mM increments. The effect of temperature on the resolution was studied within the range of 10–45°C by 5°C steps. After the optimization of all the abovementioned parameters, an optimal BGE of 40 mM phosphate buffer (pH set to 4.4) was selected for the separation, whereas the temperature of the capillary was maintained at 10°C. Applying the previously developed dual CD system and the optimal separation parameters, a resolution of 2.24 could be achieved, high enough for the determination of enantiomeric impurity. Electropherogram of the optimized system is shown in Fig. 2D.

### 3.3 NMR experiments

#### 3.3.1 The Job's method

The stoichiometry of the inclusion complex was determined with Job analysis, using 2 mM (*R*)-Sgli and 2 mM  $\beta$ -CD or 2 mM SB- $\beta$ -CD or 1:1 mM  $\beta$ - and SB- $\beta$ -CD at pH 4.2 in 30 mM phosphate buffer ( $\text{H}_2\text{O}/\text{D}_2\text{O}$ , 9/1). The stock solutions were mixed at different ratios and chemical shift changes of both the guests and the hosts were recorded. The

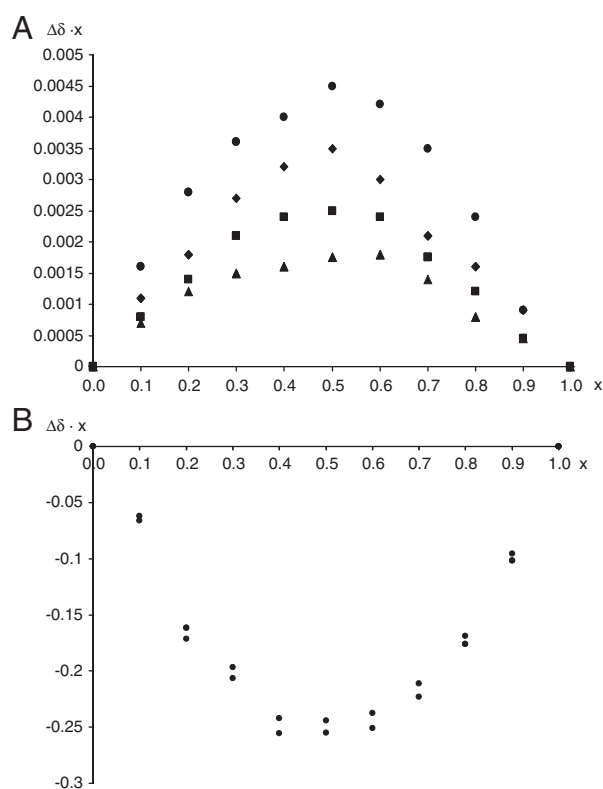


**Figure 3.** (A) Job's plot derived from the downfield changes in chemical shift of H-16 (circle) and H-4a (triangle) Sgli, and 3-H (rhombus), and 5-H  $\beta$ -CD protons (square) on a Sgli- $\beta$ -CD/SB- $\beta$ -CD dual CD sample. (B) Job's plot illustrating the upfield chemical shift changes of F-6 and F-12 Sgli resonances on a Sgli- $\beta$ -CD sample. For further details, see Section 3.3.1.

chemical shift displacements ( $\Delta\delta$ ) weighted with the molar ratio were then plotted as functions of the molar ratio (Fig. 3). The experiments were carried out using both  $^1\text{H}$  (Fig. 3A) and  $^{19}\text{F}$  NMR (Fig. 3B) experiments. The resulting Job's plots have a maximum at 0.5, indicating the 1:1 binding stoichiometry for Sgli- $\beta$ -CD, Sgli-SB- $\beta$ -CD, and Sgli-dual CD (Fig 3A) systems.

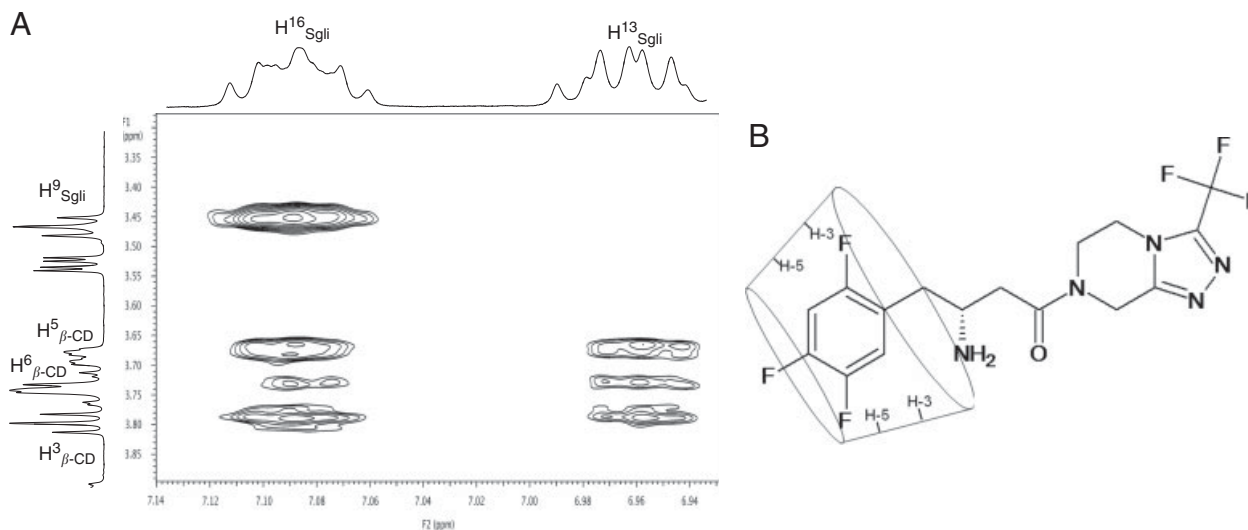


**Figure 4.** (A) Expansion of the ROESY spectrum in D<sub>2</sub>O with 300 ms mixing time, containing 3 mM (*R*)-Sgli and 3 mM β-CD showing the ROE cross-peaks between the aromatic protons of Sgli and 3-H and 5-H β-CD protons. (B) The proposed structure for the Sgli-CD inclusion complex based on the ROE cross-peaks.

### 3.3.2 2-D ROESY

To explore the structure of the inclusion complexes, 2-D ROESY NMR experiments were carried out on samples containing (*R*)-Sgli and either β-CD or SB-β-CD or β-CD/SB-β-CD dual CD system. The cross-peaks between CD and Sgli signals indicate the spatial proximity of the protons as shown in Fig. 4A. Cross-peaks between aromatic Sgli and inner CD protons can be observed in each spectrum. The most intensive cross-peaks were observed between the aromatic Sgli protons (H-13 and H-16) and the inner CD protons (3-H, 5-H). Less intensive cross-peaks between H-10 Sgli and 3-H CD protons provided additional information about the direction of inclusion and confirmed the involvement of the aromatic ring in the complexation. These data suggest that the trifluorobenzene moiety of the guest gets in the CD cavity from the wider secondary rim. The proposed structure for the Sgli-CD complex is shown in Fig. 4B.

Results of the Job plot and ROESY experiments suggest that the two CDs do not co-operate during the complex formation (averaged complex stoichiometry, 1:1). The co-operation of the CDs is limited to the chiral recognition and separation through improvement in selectivity and influence of enantiomer mobility.

## 4 Concluding remarks

An efficient and sensitive CZE method for the chiral analysis of a novel anti-diabetic drug, (*R*)-Sgli (Januvia) and its (*S*)-enantiomer was developed. The acid–base profiling of the analyte was carried out with both CE–pH and <sup>1</sup>H NMR–pH titrations resulting in p*K*<sub>a</sub> values of good agreement. The complexation behavior of (*R*)- and (*S*)-Sgli

and 30 CDs were investigated with CE under acidic conditions. Due to the less effective enantioseparation with single CDs, dual CD systems were extensively investigated. The 5 mM β-CD/5 mM SB-β-CD (DS~4) chiral selector system was found to be the best for the enantioseparation providing a resolution of *R*<sub>s</sub> = 2.24. <sup>1</sup>H and <sup>19</sup>F NMR-based Job plots unequivocally proved 1:1 Sgli-CD stoichiometry under acidic conditions. On the basis of ROESY studies, a geometric model of the inclusion complex was constructed with the trifluorobenzene moiety of Sgli and an inclusion through a wider rim of the CD.

*This work was supported by the Hungarian Scientific Research Found OTKA K73804.*

*The authors have declared no conflict of interest.*

## 5 References

- [1] Kim, D., Wang, L., Beconi, M., Eiermann, G. J., Fisher, M. H., He, H., Hickey, G. J., Kowalchick, J. E., Leitinger, B., Lyons, K., Marsilio, F., McCann, M. E., Patel, R. A., Petrov, A., Scapin, G., Patel, S. B., Roy, R. S., Wu, J. K., Wyratt, M. J., Zhang, B. B., Zhu, L., Thornberry, N. A., Weber, A. E., *J. Med. Chem.* 2005, 48, 141–151.
- [2] Drucker, D. J., *Exp. Opin. Inv. Drug* 2003, 12, 87–100.
- [3] Villhauer, E. B., Coppola, G. M., Hughes, T. W., *Annu. Rep. Med. Chem.* 2001, 36, 191–200.
- [4] Ahren, B., Schmitz, O., *Horm. Metab. Res.* 2004, 36, 867–876.
- [5] Weber, A. E., *J. Med. Chem.* 2004, 47, 4135–4141.
- [6] Zeng, W., Xu, Y., Constanzer, M., Woolf, E. J., *J. Chromatogr. B* 2010, 878, 1817–1823.

- [7] Nirogi, R., Kandikere, V., Mudigonda, K., Komarneni, P., Aleti, R., Boggavarapu, R., *Biomed. Chromatogr.* 2008, **22**, 214–222.
- [8] Clausen, M. A., Dziadul, B., Cappuccio, K. L., Kaba, M., Starbuck, C., Hsiao, Y., Dowling, T. M., *Org. Process Res. Dev.* 2006, **10**, 723–726.
- [9] Steinhuebel, D., Sun, Y., Matsumura, K., Sayo, N., Saito, T., *J. Am. Chem. Soc.* 2009, **131**, 11316–11317.
- [10] Hansen, K. B., Hsiao, Y., Xu, F., Rivera, N., Clausen, A., Kubryk, M., Krska, S., Rosner, T., Simmons, B., Balsells, J., Ikemoto, N., Sun, Y., Spindler, F., Malan, C., Grabowski, E. J. J., Armstrong, J. D., *J. Am. Chem. Soc.* 2009, **131**, 8798–8804.
- [11] Zeng, L. L., Ding, Y. J., Zhang, G. C., Song, H. R., Hu, W. H., *Chin. Chem. Lett.* 2009, **20**, 1397–1399.
- [12] Savile, C. K., Janey, J. M., Mundorff, E. C., Moore, J. C., Tam, S., Jarvis, W. R., Colbeck, J. C., Krebber, A., Fleitz, F. J., Brands, J., Devine, P. N., Huisman, G. W., Hughes, G. J., *Science* 2010, **329**, 305–309.
- [13] Juvancz, Z., Kendrovics, R. B., Iványi, R., Szente, L., *Electrophoresis* 2008, **29**, 1701–1712.
- [14] Chankvetadze, B., *Capillary Electrophoresis in Chiral Analysis*, Wiley, Chichester 1997.
- [15] Evans, C. E., Stalcup, A. M., *Chirality* 2003, **15**, 709–723.
- [16] De Boer, T., De Zeeuw, R. A., De Jong, G. J., Ensing, K., *Electrophoresis* 2000, **21**, 3220–3239.
- [17] Chankvetadze, B., *J. Chromatogr. A* 1997, **792**, 269–295.
- [18] Fillet, M., Fotsing, L., Crommen, J., *J. Chromatogr. A* 1998, **817**, 113–119.
- [19] Fillet, M., Chankvetadze, B., Crommen, J., Blaschke, G., *Electrophoresis* 1999, **20**, 2691–2697.
- [20] Schneider, H.-J., Hacket, F., Rudiger, V., Ikeda, H., *Chem. Rev.* 1998, **98**, 1755–1785.
- [21] Fielding, L., *Tetrahedron* 2000, **56**, 6151–6170.
- [22] Chankvetadze, B., *Chem. Soc. Rev.* 2004, **33**, 337–347.
- [23] Job, P., *Ann. Chim.* 1928, **9**, 113.
- [24] Béni, S., Sohajda, T., Neumajer, G., Iványi, R., Szente, L., Noszál, B., *J. Pharm. Biomed. Anal.* 2010, **51**, 842–852.
- [25] Neuhaus, D., Williamson, M. P., *The Nuclear Overhauser Effect in Structural and Conformational Analysis*, VCH, Weinheim 2000.
- [26] Sohajda, T., Varga, E., Iványi, R., Fejos, I., Szente, L., Noszál, B., Béni, S., *J. Pharm. Biomed. Anal.* 2010, **53**, 1258–1266.
- [27] Wallingford, R. A., Ewing, A. G., *Adv. Chromatogr.* 1989, **29**, 1–76.
- [28] Rundlett, K. L., Armstrong, D. W., *J. Chromatogr. A* 1996, **721**, 173–186.
- [29] King, E. J., *Acid-Base Equilibria*, Pergamon, Oxford 1965.
- [30] Gutowsky, H. S., Saika, A., *J. Chem. Phys.* 1953, **21**, 1688–1694.
- [31] Connors, K. A., *Binding Constants*, Wiley, New York 1987.
- [32] Rundlett, K. L., Armstrong, D. W., *Electrophoresis* 1997, **18**, 2194–2202.
- [33] Wren, S. A. C., Rowe, R. C., *J. Chromatogr.* 1992, **603**, 235–241.